Tides on the Ross Ice Shelf observed with ICESat

Laurie Padman[1] and Helen Amanda Fricker[2]

Received 13 April 2005; revised 20 June 2005; accepted 24 June 2005; published 29 July 2005.

[1] The Ice, Cloud and land Elevation Satellite (ICESat) provides the first opportunity for measurement of surface elevation h_i over the portions of the Antarctic ice shelves that are south of the European Remote Sensing (ERS) satellite maximum latitude (81.5°S). The dominant source of short-period variability in h_i is ocean tides. We use crossover elevation difference (Δh_i) data from the Ross Ice Shelf (RIS) to demonstrate ICESat's ability to detect the tidal signal, and to compare the accuracy of several tide models. The root-mean-square (rms) value of all RIS measurements of Δh_i is ≈0.74 m; after removing the tide using the most accurate model, the rms of the residual signal in regions of optimal model performance is ≈0.16 ± 0.03 m. This value corresponds to an uncertainty in h_i of 0.11 ± 0.02 m. We postulate that the primary sources of the residual signal are tide model errors and the inverse barometer effect. **Citation:** Padman, L., and H. A. Fricker (2005), Tides on the Ross Ice Shelf observed with ICESat, *Geophys. Res. Lett.*, *32*, L14503, doi:10.1029/2005GL023214.

1. Introduction

[2] The main processes through which mass is lost from the Antarctic ice sheet, iceberg calving and basal melting, take place in the floating ice shelves. Because they are in direct contact with both atmosphere and ocean, it is likely that ice shelves are sensitive indicators of climate change: the first signs of changing climate may be seen in these regions as enhanced surface and basal melt, and increased calving rates [*Mercer*, 1978]. Indeed, several small ice shelves of the Antarctic Peninsula have broken up over the past few years, coincident with a significant regional atmospheric warming [e.g., *Doake and Vaughan*, 1991].

[3] Satellite altimeters measure the surface elevation (h_i) of the Antarctic ice shelves to the accuracy, spatial resolution and extent required for change detection. In most locations on ice shelves, however, the largest signal in h_i is the response of the ice shelf to the ocean tides. This signal must be accurately removed before seasonal and longer-term changes in ice shelf volume and flux can be quantified [e.g., *Shepherd et al.*, 2003]. Offshore of a ~5 km zone of ice shelf flexure seaward of the grounding line, ice shelves are in isostatic balance with the ocean tide propagating in the ocean cavity beneath them. Thus, for large ice shelves, tide removal may be accomplished by ocean tidal modeling or, when sufficient data are available at a particular location, by applying tidal harmonic analyses to elevation time series.

[4] Harmonic analyses of repeat radar altimeter (RA) data from the ERS satellites (1991 to present) provide some information on ice shelf tides [*Fricker and Padman*, 2002; *Shepherd and Peacock*, 2003]. The same studies, however, found limitations in tidal analyses of ERS RA data due to its low accuracy in ice-tracking mode (~0.5 m root-mean-square (rms) error) and aliasing of several energetic tidal harmonics to inseparable low frequencies (or, in the case of the S_2 harmonic, to infinite period). Furthermore, the two largest Antarctic ice shelves, the Filchner-Ronne Ice Shelf (FRIS) in the southern Weddell Sea and the Ross Ice Shelf (RIS), extend to ~83°S and ~85.4°S, respectively, well south of the ERS maximum latitude of ~81.5°S. NASA's ICESat, which carries the Geoscience Laser Altimeter System (GLAS), has a maximum latitude of ~86°S and is the first altimeter satellite to cover the entire floating portion of the Antarctic ice sheet [*Zwally et al.*, 2002].

[5] In this paper we show that ICESat can detect the tidal signal on Antarctic ice shelves, and that the ICESat data are sufficiently accurate to identify the optimum tide model from a selection of several published models. We focus on the RIS because of ongoing interest in Siple Coast tides, and because there are several in situ tidal measurements available from the region which allow us to compare the accuracy of several published tide models independently of the ICESat data.

2. ICESat Data

[6] We used Release 19 of the GLA01 L1A Global Altimetry Data combined with Release 21 of the GLA12 Antarctica and Greenland Ice Altimetry Data from ICESat's Laser 2a 91-day operation period (40 days, 4 October–14 November 2003). In Release 21, most of the pointing biases and other errors for Laser 2a have been removed (S. B. Luthcke et al., Calibration and reduction of ICESat geolocation errors and the impact on ice sheet elevation change detection, submitted to *Geophysical Research Letters*, 2005).

[7] The elevations in the GLA12 records have had ocean tide and load tide corrections applied, using the GOT99.2 global ocean model [*Ray*, 1999]. For our analyses we require the instantaneous elevation including the tide, so we removed the applied tide corrections. To account for saturation of the GLAS detector over ice, we applied a saturation correction to the GLA12 elevations. This correction, described by H. A. Fricker et al. (Assessment of ICESat performance at salar de Uyuni, Bolivia, submitted to *Geophysical Research Letters*, 2005, hereinafter referred to as Fricker et al., submitted manuscript, 2005), uses the energy from the GLA01 corrected by a factor of 1.27 (X. Sun, personal communication, 2005). We filtered the data using ice sheet filters (B. E. Smith et al., Recent elevation changes on the ice streams and ridges of the Ross Embayment from ICESat crossovers, submitted to *Geophys-*

[1]Earth & Space Research, Corvallis, Oregon, USA.
[2]Institute of Geophysics and Planetary Physics, Scripps Institution of Oceanography, University of California, San Diego, La Jolla, California, USA.

0094-8276/05/2005GL023214$05.00

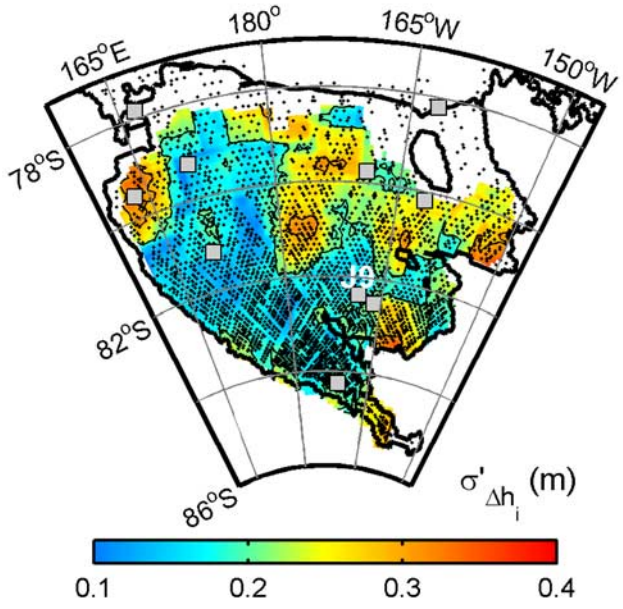

Figure 1. Location of tide elevation information for the Ross Ice Shelf. Small black dots show locations of all ICESat crossovers from the Laser 2a operation period (4 October to 14 November 2003) after a cloud filter has been applied, and excluding points within ~10 km of the grounding line. Filled gray squares are locations of gravimeter tidal records [*Williams and Robinson*, 1980]. Site J9, near 82.4°S, 191.4°E, is indicated. The grounding line, coast and ice shelf front used in the RIS_2002 model are indicated by thick black lines. Color shading shows $\sigma'_{\Delta h_i}$ (m) for RIS_2002 for overlapping regions 5° longitude × 1° latitude, evaluated at 0.5° × 0.1° spacing. Only boxes with >25 crossovers are shaded. Thin black contours indicate $\sigma'_{\Delta h_i}$ = 0.2 and 0.3 m.

ical Research Letters, 2005) so that most returns affected by cloud and other invalid returns were removed. There are about 3000 remaining crossovers on the floating portion of the RIS, with locations shown in Figure 1. Crossover density increases significantly towards ICESat's maximum latitude (~86°S). At each crossover we calculated the elevation difference $\Delta h_i(x, y) = h_i(x, y, t_2) - h_i(x, y, t_1)$, where t_1 and t_2 are the times at which the ascending and descending orbits acquired data at that location. The time separation, $\Delta t = t_2 - t_1$, ranged from <1 day to ~40 days with a mean of ~12.7 days.

3. In Situ Tide Elevation Data

[8] We used tidal coefficients from ten records of in situ tide elevation from the RIS, nine gravimeter records of 30–58 day duration and one longer (1 – y) record from McMurdo (Ross Is.) [*Williams and Robinson*, 1980]. Locations are shown in Figure 1. Our primary use of these records is to determine the accuracy of tide models.

4. Tide Models

[9] We compared six ocean tide models with in situ and ICESat data: the dynamics-based ("forward") Circum-Antarctic Tidal Simulation version 02.01 (CATS02.01) [*Padman et al.*, 2002]; a Ross Sea inverse model (RIS_2002) [*Padman et al.*, 2003] which assimilates tidal harmonics from the RIS gravimeter records; the Ross Sea Tidal Inverse Model (RossTIM), which assimilates open-shelf velocity data but not tide elevations [*Erofeeva et al.*, 2005]; the TPXO6.2 global data assimilation model, an updated version of the model reported by *Egbert and Erofeeva* [2002]; the FES 2004 global model (F. Lefèvre, personal communication, 2005); and the GOT99.2 global model presently applied in the ICESat data files [*Ray*, 1999]. The primary data constraint on the TPXO6.2 inverse model is TOPEX/Poseidon radar altimetry between ~±66°; however, the model includes a patch for the Ross Sea based on assimilation of the ten RIS gravimeter records (G. Egbert, personal communication, 2004). For the RIS it is, therefore, similar to RIS_2002, differing only by parameters used in the assimilation, including model grid spacing and coherence length scales. The FES 2004 model has a significantly different grounding line for the eastern RIS than that used by the other models.

5. Results

5.1. Model Comparison With Tidal Harmonics From Gravimeter Records

[10] At each location (x_i, y_i) where we have tidal harmonics from in situ data, we define the deviation variance

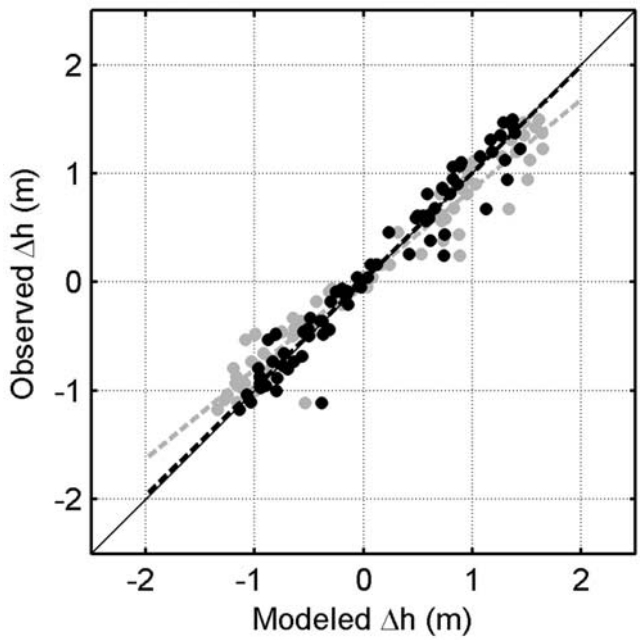

Figure 2. Comparisons of Δh_i^{obs} and Δh_i^{mod} for a circle 50 km radius surrounding site J9 (~82.4°S, 191.4°E, north of Crary Ice Rise) for two tide models, the dynamics-based CATS02.01 (gray symbols) and the inverse model RIS_2002 (black symbols). The solid diagonal line indicates perfect agreement. The dashed gray and black lines are linear least squares fits for CATS02.01 and RIS_2002, respectively. Fit statistics for these and other models are given in Table 2.

Table 1. Ensemble rms Error E_X in cm (See Text) Between Data and Tide Models for Constituents $X = \{O_1, K_1, M_2, S_2\}$ and the Multi-Constituent Value (E_{Tot}) for the 10 Gravimeter Records [*Williams and Robinson*, 1980] From the RIS, Using $c = 1.15$ in Equation (3)[a]

	O_1	K_1	M_2	S_2	E_{Tot}
RIS_2002	3.4	3.2	2.0	2.2	6.3
TPXO6.2	2.3	3.2	3.8	2.0	6.6
CATS02.01	4.0	6.5	2.0	5.0	10.7
FES 2004	6.2	4.9	4.8	2.4	10.8
GOT99.2	4.9	6.6	5.5	4.6	12.5
RossTIM	6.9	8.9	2.4	5.0	14.4

[a]Models are ranked by increasing E_{Tot}.

for harmonic X, with observed (modeled) amplitude and phase $a^{obs}_{i,X}$ ($a^{mod}_{i,X}$) and $p^{obs}_{i,X}$ ($p^{mod}_{i,X}$) as:

$$d^2_{i,X} = \frac{1}{2}\left(a^{obs}_{i,X}\cos\left(p^{obs}_{i,X}\right) - a^{mod}_{i,X}\cos\left(p^{mod}_{i,X}\right)\right)^2 + \left(a^{obs}_{i,X}\sin\left(p^{obs}_{i,X}\right) - a^{mod}_{i,X}\sin\left(p^{mod}_{i,X}\right)\right)^2. \quad (1)$$

The ensemble-averaged rms deviation for a set of N tidal stations is given by

$$E_X = \left(\frac{1}{N}\sum\nolimits_i d^2_{i,X}\right)^{1/2}, \quad (2)$$

and an ensemble value for multiple constituents is defined as

$$E_{Tot} = c\left(\sum\nolimits_X E^2_X\right)^{1/2}. \quad (3)$$

In (3), c is a scale factor relating the total rms value to the value determined from the summation of a limited set of constituents. Based on calculations of the rms tide height from the RIS_2002 model, $c \approx 1.15$ for relating a full tidal solution to the value from summing over only O_1, K_1, M_2, and S_2. Comparisons of E_X and E_{Tot} for the six tide models (Table 1) show that, as expected, those which assimilate the gravimetric data (RIS_2002 and TPXO6.2) perform best in comparison with the same data. The remaining errors with the assimilation models ($E_{Tot} \approx 0.06$ m) represent our uncertainty in the coefficients from the gravimeter records, due to measurement error and short record length (<2 months except for the McMurdo station). A previous study of RIS tides [*Padman et al.*, 2003] demonstrated that RIS_2002 provided a better model fit than the forward model CATS02.01 to independent (unassimilated) elevation differences from SAR interferometry. We therefore anticipate that ICESat crossover data will also be more accurately modeled by RIS_2002 and TPXO6.2 than by the other models.

5.2. Model Comparison With ICESat Crossover Data

[11] There are no in situ RIS elevation data coincident in time with the ICESat Laser 2a operation period. Furthermore, there are insufficient ICESat crossovers close to each gravimeter site to do a direct comparison with gravimeter-based tide predictions at these points. Instead, we compare the ICESat crossover values with predicted values from each tide model. For the assimilation models RIS_2002 and TPXO6.2, this approach can be thought of as using the models' dynamical equations to interpolate and extrapolate $a^{obs}_{i,X}$ and $p^{obs}_{i,X}$ from the gravimeter sites throughout the RIS.

[12] For each tide model, we calculated sets of modeled values of the crossover elevation differences $\Delta h_i^{mod}(x, y, t_1, t_2)$, to compare with the observed values ($\Delta h_i^{obs}(x, y, t_1, t_2)$) from ICESat. In our predictions, we include corrections for the long-period (~18.6 y) node-tide modulation and inference of minor tides from the major modeled harmonics. The models predict the ocean tide, i.e., the surface elevation relative to the seabed, whereas the altimeter-derived elevation includes the contribution from the load tide, i.e., the deflection of the solid earth due to the tidal contribution to the total weight of water above it. We use a model based on TPXO6.2 to correct $\Delta h_i^{obs}(x, y, t_1, t_2)$ for the load tide, evaluated for each tidal harmonic following *Ray* [1998].

[13] We evaluated the ability of each tide model to represent the variability in ICESat elevation data using three statistical quantities: (1) the rms of the difference between Δh_i^{mod} and Δh_i^{obs}, denoted $\sigma'_{\Delta h_i}$; (2) the correlation coefficient, r, between these values; and (3) the slope, m, of the linear least squares best fit for $\Delta h_i^{obs} = m\Delta h_i^{mod} + offset + error$. A value of $m < 1$ ($m > 1$) implies that the real tide range is smaller (greater) than the modeled range. Altimeter data within 10 km of the grounding line were excluded from the analysis since the assumption that shelf ice is fully hydrostatically supported by the ocean is not valid within the grounding zone. We first compared Δh_i^{mod} with Δh_i^{obs} for a small region of the RIS, a circle with 50-km radius centered on 82.4°S, 191.4°E, near site J9 north of Crary Ice Rise (see Figure 1). This region was chosen because assimilation of the two nearby gravimeter records should significantly improve the RIS_2002 and TPXO6.2 models relative to the other models. The values of $\sigma'_{\Delta h_i}$, r and m for all models are listed in Table 2. A graphical comparison for the forward CATS02.01 and inverse RIS_2002 models (Figure 2) shows that the variability in Δh_i^{obs} is strongly correlated with predicted tidal displacements. For site J9, $\sigma'_{\Delta h_i}$ varies between 0.18 and 0.32 m, and m varies from 0.76 to 1.23. The value of m is much closer to unity for RIS_2002 than for CATS02.01; i.e., in this location, ICESat data are successful in identifying the tide model (RIS_2002) which is known to be more accurate through comparisons with in situ data.

[14] Fit statistics calculated for the entire RIS as a single group confirm that the elevation assimilation models RIS_2002 and TPXO6.2 have the lowest values of $\sigma'_{\Delta h_i}$ and comparable magnitudes of $|m - 1|$ (Table 2). The RossTIM model performs poorly at site J9 and for

Table 2. Statistics for Fits Between Modeled and Measured Elevation Differences, Δh_i^{mod} and Δh_i^{obs}, at ICESat Crossovers on the Ross Ice Shelf (RIS), for Six Tide Models Identified in the Text[a]

	J9			RIS		
	$\sigma'_{\Delta h_i}$	r	m	$\sigma'_{\Delta h_i}$	r	m
RIS_2002	0.18	0.98	0.99	0.22	0.95	0.95
TPXO6.2	0.24	0.96	1.14	0.22	0.94	1.04
CATS02.01	0.24	0.98	0.82	0.26	0.94	0.86
FES 2004	0.21	0.97	1.12	0.33	0.88	1.01
GOT99.2	0.32	0.93	1.23	0.29	0.92	1.08
RossTIM	0.30	0.97	0.76	0.27	0.94	0.83

[a]See text for explanations of $\sigma'_{\Delta h_i}$(m), r and m. Statistics are reported for a circle 50-km radius around site J9 (~82.4°S; 191.4°E) north of Crary Ice Rise, and for the entire RIS. The rms values of Δh_i^{obs}, prior to tide removal, were 0.81 m and 0.74 m for J9 and RIS, respectively.

the entire RIS. The FES 2004 model performs well near J9 but has high $\sigma'_{\Delta h_i}$ for the entire RIS, a result which we attribute to incorrect specification of the Siple Coast grounding line. The GOT99.2 model (the model provided in the ICESat data files) performs poorly at both J9 and for the entire RIS, as is also seen in model comparisons with in situ data (Table 1).

[15] The spatial distribution of $\sigma'_{\Delta h_i}$ over the entire RIS for the optimum model (RIS_2002) demonstrates generally good performance but with some areas of higher $\sigma'_{\Delta h_i}$, primarily along the Siple Coast (Figure 1). For Figure 1, fit statistics were calculated for overlapping regions extending 5° in longitude by 1° in latitude (~100 km × ~100 km). This box size was chosen to provide a sufficient number of crossovers (>25) in each box for calculation of statistics. The typical value of $\sigma'_{\Delta h_i}$ is ~0.16 ± 0.03 m in regions of apparently good tide model accuracy near assimilated gravimetry sites, away from the Siple Coast (Table 2 and Figure 1). Since the error of Δh_i^{obs} is $\sim\sqrt{2}$ times the error of each elevation estimate (h_i) in the pair, the equivalent rms error of h_i is $\sigma'_{\Delta h_i}$ = 0.11 ± 0.02 m in these regions.

6. Discussion and Conclusions

[16] ICESat extends satellite altimeter coverage to the southern regions of the RIS and the Filchner-Ronne Ice Shelf, including the grounding zones of the southern Siple Coast ice streams in the eastern RIS and Foundation Ice Stream feeding the southern FRIS. The variance of ICESat crossover elevation difference values (Δh_i^{obs}) for the entire RIS is $\sigma^2_{\Delta h_i} \approx 0.74^2$ m^2 for the 40-day record from the Laser 2a operation period. The ice shelf response to ocean tides accounts for >90% of this variance. The ICESat data allow us to identify the most accurate tide model from a set of models available for Ross Sea tide prediction. As expected, models in which nearby in situ tide elevation data have been assimilated (RIS_2002 and TPXO6.2) perform significantly better, in comparisons with ICESat data, than models which have no local data constraints. The latter include GOT99.2, which is the model presently provided with the ICESat data products.

[17] After removing the tide predicted by the most accurate tide model (RIS_2002), the rms height difference at crossovers is $\sigma'_{\Delta h_i} \approx 0.16 \pm 0.03$ m for ~50% of the area of the RIS. This value corresponds to a deviation for an individual ICESat altimeter estimate (h_i) of σ'_{h_i} = 0.11 ± 0.02 m. We interpret this value as the approximate accuracy currently available from ICESat for these portions of the RIS. The value of σ'_{h_i} is much greater than the ~0.03 m shot-to-shot accuracy determined for ICESat from studies at salar de Uyuni (*Fricker et al.*, submitted manuscript, 2005). The primary contributors to $\sigma_{h_i}{}'$ for the RIS are believed to be remaining tide model errors and the inverse barometer effect (IBE). We estimate the rms error in inverse models as ~0.05 m near in situ data points (see Table 1), but it may be higher elsewhere (see following paragraph). The IBE is an elevation change associated with atmospheric pressure variability, at a rate of ~−1 cm per hPa, and has a typical rms signal over Antarctic ice shelves of ~0.08 m [*Padman et al.*, 2004]. Other sources of h_i variance include residual ICESat errors due to pointing, saturation and cloud cover, and geophysical changes that have not been accounted for, e.g., snow accumulation, firn compaction, basal melt, and advection. The latter three terms are expected to be small since the mean time separation of points in each crossover is only ~13 days; however, the influence of snowfall and drift on these time-scales may be significant.

[18] We interpret large values of $\sigma'_{\Delta h_i}$ (>0.2 m) in Figure 1 as indicating that even the optimum tide model performs poorly in those regions. The largest values are along the eastern and western grounding lines. We hypothesize that the primary causes of model inaccuracy are errors in (*i*) the sub-ice-shelf water column thickness (w.c.t.) and (*ii*) frictional energy loss parameterizations in the shallow water equations, which are used to dynamically extrapolate the influence of assimilated data points throughout the RIS_2002 domain. We anticipate further improvements in tide model accuracy from amendments to the w.c.t. grid, motivated by seeking model agreement with ICESat and recently obtained in situ elevation data along the Siple Coast. Preliminary analyses also indicate that the high along-track resolution of ICESat (~172 m between shots) can be used to improve our definition of the grounding line, another significant source of error in existing Antarctic tide models and other ice shelf modeling studies.

[19] **Acknowledgments.** We thank the ICESat Science Project and the NSIDC for distribution of the ICESat data (see http://icesat.gsfc.nasa.gov and http://nsidc.org/data/icesat/). Work at ESR was funded by NASA grant NAG5-7790 and the NSF Office of Polar Programs (OPP-0125602), and work at SIO was funded by NASA contract NAS5-99006. We thank F. Lefèvre for providing the most recent release of FES 2004. Comments by two anonymous reviewers contributed significantly to the clarity of this manuscript. This is ESR contribution number 91.

References

Doake, C. S. M., and D. G. Vaughan (1991), Rapid disintegration of Wordie Ice Shelf in response to atmospheric warming, *Nature*, *350*, 328–330.

Egbert, G. D., and S. Y. Erofeeva (2002), Efficient inverse modeling of barotropic ocean tides, *J. Atmos. Oceanic Technol.*, *19*(2), 183–204.

Erofeeva, S. Y., G. D. Egbert, and L. Padman (2005), Assimilation of ship-mounted ADCP data for barotropic tides: Application to the Ross Sea, *J. Atmos. Oceanic Technol.*, *22*(6), 721–734.

Fricker, H. A., and L. Padman (2002), Tides on Filchner-Ronne Ice Shelf from ERS radar altimetry, *Geophys. Res. Lett.*, *29*(12), 1622, doi:10.1029/2001GL014175.

Mercer, J. H. (1978), West Antarctic ice sheet and CO_2 greenhouse effect: A threat of disaster, *Nature*, *271*, 321–325.

Padman, L., H. A. Fricker, R. Coleman, S. Howard, and S. Erofeeva (2002), A new tide model for the Antarctic ice shelves and seas, *Ann. Glaciol.*, *34*, 247–254.

Padman, L., S. Erofeeva, and I. Joughin (2003), Tides of the Ross Sea and Ross Ice Shelf, *Antarct. Sci.*, *15*(1), 31–40.

Padman, L., M. King, D. Goring, H. Corr, and R. Coleman (2004), Ice shelf elevation changes due to atmospheric pressure variations, *J. Glaciol.*, *49*(167), 521–526.

Ray, R. D. (1998), Ocean self-attraction and loading in numerical tidal models, *Mar. Geod.*, *21*, 181–192.

Ray, R. D. (1999), A global ocean tide model from TOPEX/Poseidon altimetry: GOT99.2, *NASA Tech. Memo., 209478*, 58 pp.

Shepherd, A., and N. R. Peacock (2003), Ice shelf tidal motion derived from ERS altimetry, *J. Geophys. Res.*, *108*(C6), 3198, doi:10.1029/2001JC001152.

Shepherd, A., D. Wingham, T. Payne, and P. Skvarca (2003), Larsen ice shelf has progressively thinned, *Science*, *302*(5646), 856–859.

Williams, R. T., and E. S. Robinson (1980), The ocean tide in the southern Ross Sea, *J. Geophys. Res.*, *85*, 6689–6696.

Zwally, H. J., et al. (2002), ICESat's laser measurements of polar ice, atmosphere, ocean and land, *J. Geodyn.*, *34*, 405–445.

H. A. Fricker, Institute of Geophysics and Planetary Physics, Scripps Institution of Oceanography, University of California, San Diego, La Jolla, CA 92093-0225, USA.

L. Padman, Earth & Space Research, 3350 SW Cascade Avenue, Corvallis, OR 97333-1536, USA. (padman@esr.org)